

Universality of random-site percolation thresholds for two-dimensional complex non-compact neighborhoods

Krzysztof Malarz*

AGH University, Faculty of Physics and Applied Computer Science, al. Mickiewicza 30, 30-059 Kraków, Poland
(Dated: February 13, 2024)

The phenomenon of percolation is one of the core topics in statistical mechanics. It allows one to study the phase transition known in real physical systems only in a purely geometrical way. In this paper, we determine thresholds p_c for random site percolation in triangular and honeycomb lattices for all available neighborhoods containing sites from the sixth coordination zone. The results obtained (together with the percolation thresholds gathered from the literature also for other complex neighborhoods and also for a square lattice) show the power-law dependence $p_c \propto (\zeta/K)^{-\gamma}$ with $\gamma = 0.526(11)$, $0.5439(63)$ and $0.5932(47)$, for honeycomb, square, and triangular lattice, respectively, and $p_c \propto \zeta^{-\gamma}$ with $\gamma = 0.5546(67)$ independently on the underlying lattice. The index $\zeta = \sum_i z_i r_i$ stands for an average coordination number weighted by distance, that is, depending on the coordination zone number i , the neighborhood coordination number z_i and the distance r_i to sites in i -th coordination zone from the central site. The number K indicates lattice connectivity, that is, $K = 3, 4$ and 6 for the honeycomb, square and triangular lattice, respectively.

Keywords: random site percolation; Archimedean lattices; Newman–Ziff algorithm; complex and extended neighborhoods; analytical formulas for percolation thresholds; Monte Carlo simulation

I. INTRODUCTION

The percolation [1–4] is one of a core topics in statistical physics as it allows for studying phase transitions and their properties in only geometrical fashion, i.e., without heating or cooling anything (except of paying unconscionable invoices for electricity in the computer centers). Although originated from a rheology [5, 6] (and still applied there [7]) the application of percolation theory range from forest fires [8] to disease propagation [9], not omitting problems originated in hard physics (including magnetic [10] and electric [11] properties of solids) but also with implications for: nanoengineering [12]; materials chemistry [13]; agriculture [14]; sociology [15]; terrorism [16]; urbanization [17]; dentistry [18]; information transfer [19]; computer networks [20]; psychology of motivation [21]; and finances [22] (see References 23–25 for the most recent reviews also on fractal networks [26] or explosive percolation [27]).

The phase transition mentioned above is first of all characterized by a critical parameter called *percolation threshold* p_c and much effort went into searching for a universal formula that allows for the prediction p_c based solely on the scalar characteristics of a lattice or a network topology, where the percolation phenomenon occurs. Probably, searching for such dependencies is not different much from searching for the alchemic formula for the philosopher’s stone—allowing for converting anything (or at least something) into gold. Anyway, such attempts of proposing universal formula for percolation threshold were more or less successfully made earlier.

For instance, Galam and Mauger [28] proposed an uni-

versal formula

$$p_c = \frac{p_0}{[(d-1)(z-1)]^a} \quad (1a)$$

depending on the connectivity of the lattice z and its dimension d . For a site percolation problem they identified two groups of lattices, i.e., two sets of parameters p_0 and a . Their paper was immediately criticized by van der Marck [29, 30] who indicated two lattices with identical z and d but different values of p_c associated with these lattices. For two-dimensional lattices the Galam–Mauger formula reduces to

$$p_c = \frac{p_0}{(z-1)^a}, \quad (1b)$$

with $p_0 = 0.8889$ and $a = 0.3601$ for triangular, square and honeycomb lattices [28]. Their studies were extended to anisotropic lattices without equivalent nearest neighbors, non-Bravais lattices with two atom unit cells, and quasicrystals which required the substitution of z in Equation (1) by an effective (non integer) value z_{eff} [31, 32].

Very recently, Xun *et al.* [33] in extensive numerical simulations showed that all Archimedean lattices (uniform tilings, i.e., lattices built of repeatably sequences of tails of regular polygons able to cover a two-dimensional plane) exhibit a simple relation

$$p_c = c_1/z, \quad (2a)$$

which due to finite size effects should be modified by constant term b

$$p_c = c_2/z - b. \quad (2b)$$

For example, for the square lattice and extended compact neighborhoods, these constants are $c_2 = 4.527$ and $b =$

*  0000-0001-9980-0363; malarz@agh.edu.pl

3.341 [34]. In two dimensions, for Archimedean lattices up to the 10-th coordination zone [33], correlations are also seen by plotting

$$z \text{ versus } -1/\ln(1-p_c). \quad (3)$$

Yet another investigated by Galam and Mauger [35, 36] formulas included

$$p_c = 1/\sqrt{z-1} \quad (4)$$

or by Koza *et al.* [37, 38]

$$p_c = 1 - \exp(d/z). \quad (5)$$

The formula (2a) works well also for distorted lattices [39, 40], where lattice distortion means random moving of lattice nodes not too far from their regular position in non-distorted lattices. In this case, the number of sites in the neighborhood z should be replaced by an average site degree \bar{z} [41].

The studies mentioned above were concentrated in compact neighborhoods. When holes in the neighborhoods are taken into account, there is a strong degeneration of p_c on total z , and Equations (1) to (5)—which depend solely on the lattice dimension d and connectivity z —must fail. To avoid this $p_c(z)$ degeneracy in the case of triangular lattice, a weighted square distance

$$\xi = \sum_i r_i^2 z_i / i \quad (6)$$

was proposed, where z_i is the number of sites in the given neighbourhood in i -th coordination zone and these sites distance to the central site in neighbourhood is r_i [42]. Unfortunately, the clear dependence

$$p_c \propto \xi^{-\gamma} \quad (7)$$

(with $\gamma_{\text{TR}}^{\xi} \approx 0.710(19)$) is lost for the honeycomb lattice [43]. Thus, instead, the weighted coordination number

$$\zeta = \sum_i z_i r_i \quad (8)$$

was proposed [43] which gives a nice power law

$$p_c \propto \zeta^{-\gamma} \quad (9)$$

with $\gamma_{\text{HC}}^{\zeta} \approx 0.4981(90)$. As $\gamma_{\text{HC}}^{\zeta}$ is very close to $\frac{1}{2}$ also the dependence

$$p_c = c_3/\sqrt{\zeta} \quad (10)$$

was checked yielding $c_3 \approx 1.2251(99)$ [43].

Very recently, we tested formulas (7) and (9) also for the square lattice up to the sixth coordination zone and found that Eq. (9) also holds for a square lattice with $\gamma_{\text{SQ}}^{\zeta} \approx 0.5454(60)$ [44].

Our results show that for all three (square, triangular, and honeycomb) lattice shapes, the power law is recovered in dependence of $p_c(\zeta/K)$, where K is the connectivity of the network with the nearest-neighbour interaction, that is, with $K = 3, 4$ and 6 for the honeycomb, square, and triangular lattice, respectively. On the other hand, independent of the lattice topology, we see a more or less clear power law $p_c(\zeta)$ for the data obtained on the values of p_c for the three lattices with complex neighbourhoods containing sites up to the sixth coordination zone.

II. METHODOLOGY

In this paper—using exactly the same methodology as that used to study percolation in a square lattice with complex neighborhoods that contain sites up to the sixth coordination zone [44]—we extend our previous studies for sites up to the sixth coordination zone for triangular (Figure 1) and honeycomb (Figure 2) lattices. Namely, using the fast Monte Carlo scheme proposed by Newman and Ziff [45] and the finite-size scaling theory [46, 47] we found 64 values of percolation thresholds for complex neighborhoods containing sites from the sixth coordination zone.

In Supplemental Material [48] the mapping of the 6th coordination zone in the honeycomb lattice into the brick-wall-like square lattice (as proposed in Reference 49) is presented in Figure 1 in Appendix A together with Listing 1 (for TR-6 neighborhood) and Listing 2 (for HC-6 neighborhood) showing implementations of `boundaries()` functions to be replaced in original Newman–Ziff algorithm [45]. The mapping of the 1st to 5th coordination zones in the honeycomb lattice into the brick-wall-like square lattice are presented in Figure 3 in Reference [43].

III. RESULTS

In Figure 3 we present examples of results used to predict the percolation thresholds p_c , that is,

- the dependencies of the size of the largest cluster S_{max}/L^2 normalized to the lattice size vs. number of occupied sites also normalized to the lattice size [Figures 3(a) and 3(c)]
- and the dependencies of the probability that a randomly selected site belongs to the largest cluster, scaled by $L^{\beta/\nu}$ vs. occupation probability p [Figures 3(b) and 3(d)]

¹ For the problem of site percolation, the critical values of the exponents $\beta = \frac{5}{36}$ and $\nu = \frac{4}{3}$ are known exactly [1, p. 54].

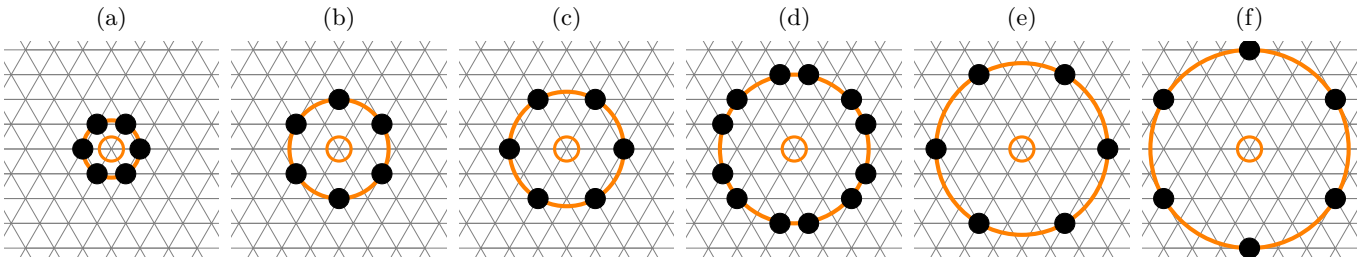


FIG. 1: Basic neighborhoods corresponding to subsequent coordination zones $i = 1, \dots, 6$ in the triangular lattice. The symbol r stands for the Euclidean distance of the black sites from the central one, and z indicates the number of sites in the neighborhood. (a) TR-1: $i = 1, r^2 = 1, z = 6$, (b) TR-2: $i = 2, r^2 = 3, z = 6$, (c) TR-3: $i = 3, r^2 = 4, z = 6$, (d) TR-4: $i = 4, r^2 = 7, z = 12$, (e) TR-5: $i = 5, r^2 = 9, z = 6$, (f) TR-6: $i = 6, r^2 = 12, z = 6$.

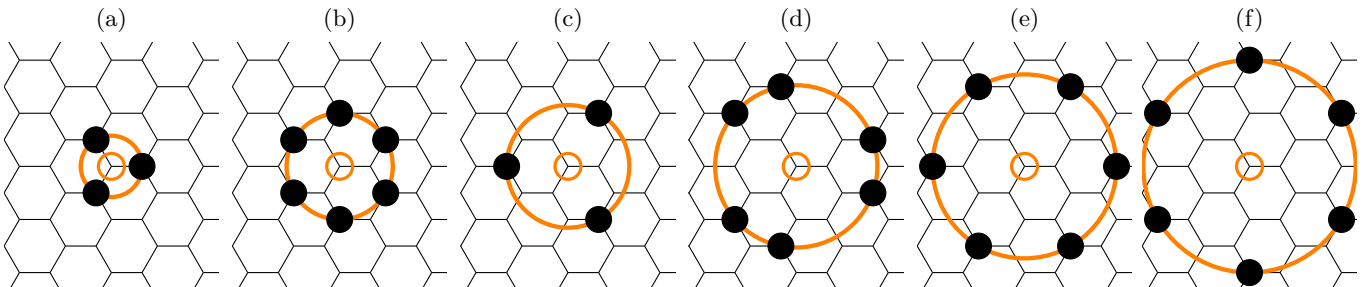


FIG. 2: Basic neighborhoods corresponding to subsequent coordination zones $i = 1, \dots, 6$ on the honeycomb lattice. The symbol r stands for the Euclidean distance of the black sites from the central one, and z indicates the number of sites in the neighborhood. (a) HC-1: $i = 1, r^2 = 1, z = 3$. The lattices (b) HC-2: $i = 2, r^2 = 3, z = 6$, (e) HC-5: $i = 5, r^2 = 9, z = 6$ and (f) HC-6: $i = 6, r^2 = 12, z = 6$ are equivalent to a triangular lattice TR-1 [Figure 1(a)] with enlarged lattice constants $\sqrt{3}$, 3 and $2\sqrt{3}$ times, respectively. (d) HC-4: $i = 4, r^2 = 7, z = 6$. The lattice (c) HC-3 ($i = 3, r^2 = 4, z = 3$), is equivalent to HC-1 [Figure 2(a)] with a lattice constant twice larger than for HC-1

for triangular (Figures 3(a) and 3(b)) and honeycomb (Figures 3(c) and 3(d)) lattice and neighbourhoods containing all considered basic neighbourhoods presented in Figure 1 (for the triangular lattice) and Figure 2 (for the honeycomb lattice). The linear sizes L of the simulated systems range from 127 to 4096 and the results of these simulations are averaged over $R = 10^5$ samples. All dependencies $\mathcal{P}_{\max} \cdot L^{\beta/\nu}$ vs. p studied here are presented in Figure 2 (for the triangular lattice) and Figure 3 (for the honeycomb lattice) in Appendix C in the Supplemental Material [48]. The common point of the curves $\mathcal{P}_{\max} \cdot L^{\beta/\nu}$ vs. p for various system sizes L predicts p_c . The computed values of p_c , associated with various neighborhoods, together with their uncertainties (also estimated earlier for neighborhoods containing sites up to the sixth coordination zone—for square lattice [44, 50, 51] and the fifth coordination zone—for triangular [42, 52] and honeycomb [43] lattices) are collected in Table I in Appendix B in the Supplemental Material [48].

Figure 4 presents the p_c for neighborhoods containing sites up to the sixth coordination zone on square (\square), honeycomb (\circ) and triangular (\triangle) lattices as dependent on

- total coordination number z [Figure 4(a)];

- index ζ [Figure 4(b)];
- index ζ/K [Figure 4(c)].

The crosses (\times) indicates inflated neighborhoods, that is, non-compact neighborhoods reducible to other complex neighborhoods by shrinking the lattice constants. Three examples of inflated neighborhood are presented in Figure 5. The detected inflated neighborhoods and their lower index equivalents are presented in Table I. These values p_c are excluded from the fitting procedure.

As we mentioned in the Introduction, for complex non-compact neighborhoods, strong $p_c(z)$ degeneration is observed [see Figure 4(a)]. On the contrary, introducing the index ζ (8) allows a nearly perfect separation of the values of p_c . After excluding inflated neighborhoods (presented in Table I) the linear fit of the data presented in Figure 4(c) with the least-squares method gives in the power law

$$p_c \propto (\zeta/K)^{-\gamma} \quad (11)$$

exponents $\gamma_{\text{TR}} = 0.5932(47)$, $\gamma_{\text{sq}} = 0.5439(63)$, $\gamma_{\text{HC}} = 0.526(11)$, for triangular, square and honeycomb lattices, respectively. The analogous fit according to Equation (9) of the data presented in Figure 4(b) gives the exponent $\gamma_{2\text{D}} = 0.5546(67)$.

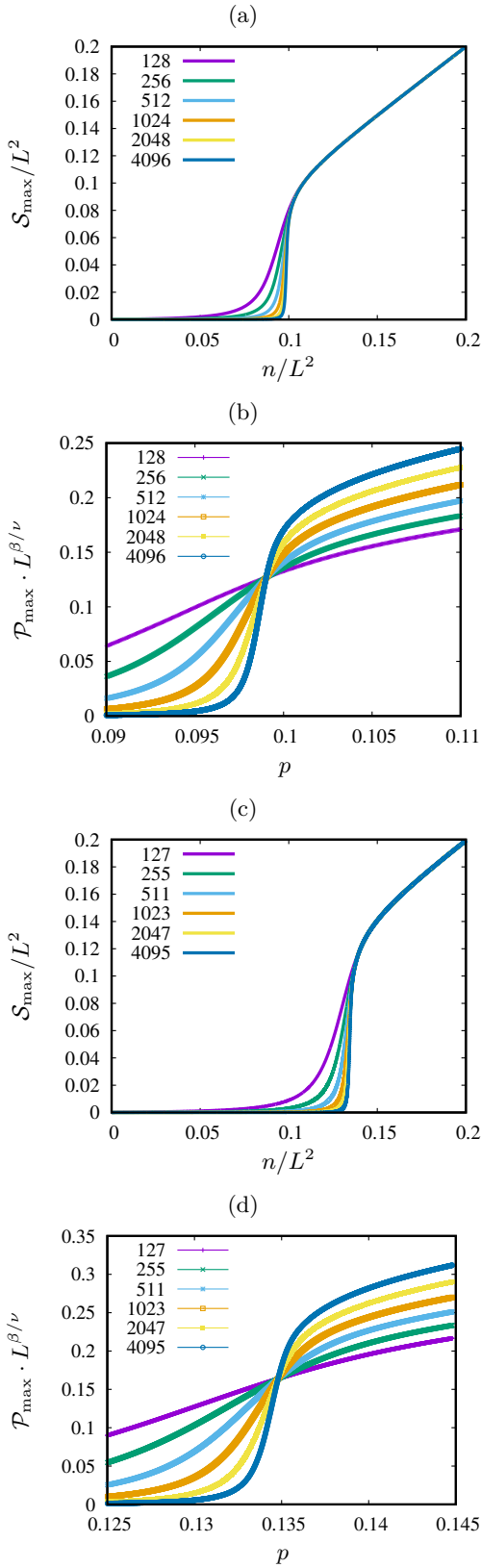


FIG. 3: Examples of [(a) and (c)] S_{\max}/L^2 versus n/L^2 and [(b) and (d)] $\mathcal{P}_{\max} \cdot L^{\beta/\nu}$ versus p for [(a) and (b)] TR-1,2,3,4,5,6 and [(c) and (d)] HC-1,2,3,4,5,6 neighborhoods

TABLE I: Detected inflated (together with the associated ζ index) and equivalent neighborhoods. The percolation thresholds p_c and total number of sites z are common for both neighborhoods.

inflated neighborhood	ζ	p_c	z	equivalent neighborhood
SQ-2	5.6568	0.5927	4	SQ-1
SQ-3	8	0.5927	4	SQ-1
SQ-5	11.3137	0.5927	4	SQ-1
SQ-6	12	0.5927	4	SQ-1
SQ-2,3	13.6568	0.4073	8	SQ-1,2
SQ-2,5	16.9705	0.337	8	SQ-1,3
SQ-3,5	19.3137	0.4073	8	SQ-1,2
SQ-2,3,5	24.9705	0.288	12	SQ-1,2,3
TR-2	10.3923	0.5	6	TR-1
TR-3	12	0.5	6	TR-1
TR-5	18	0.5	6	TR-1
TR-6	20.7846	0.5	6	TR-1
TR-2,5	28.3923	0.29028	12	TR-1,2
TR-2,6	31.1769	0.26455	12	TR-1,3
TR-3,6	32.7846	0.29030	12	TR-1,2
TR-5,6	38.7846	0.23200	12	TR-2,3
TR-2,5,6	49.1769	0.21550	18	TR-1,2,3
HC-2	10.3923	0.5	6	TR-1
HC-3	6	0.697	3	HC-1
HC-5	15.5884	0.5	6	TR-1
HC-6	20.7846	0.5	6	TR-1
HC-2,5	28.3923	0.29028	12	TR-1,2
HC-2,6	31.1769	0.26453	12	TR-1,3
HC-3,6	26.7846	0.36301	9	HC-1,2
HC-5,6	38.7846	0.23202	12	TR-2,3
HC-2,5,6	49.1769	0.21547	18	TR-1,2,3

IV. DISCUSSION

The introduction of the ζ index solves the problem of multiple degeneration of the value of p_c . Eliminating inflated neighborhoods (including those that occur pairwise between a triangular and a hexagonal lattice) allows fitting p_c to the power laws according to Equations (9) or (11). Without comparing the hexagonal and triangular lattices, it was necessary to introduce the index ξ to maintain the power law relationship according to Equation (7). The index ξ turned out to be redundant vs. ζ index for the site percolation problem, because previously outlier points turned out to belong to the inflated neighborhoods, but the low-index neighborhoods associated with them were located on a different type of lattice. However, the introduction of the index ξ turned out to be quite useful for the bond percolation problem, where the relationship (7) is perfectly satisfied with the exponent $\gamma \approx 1$ [53].

Finally, we propose some unification of the nomenclature appearing in the literature, and applying terms:

basic neighborhoods: for those containing sites from a single coordination zone (like SQ-1, SQ-2, SQ-3, etc. and those presented in Figures 1 and 2);

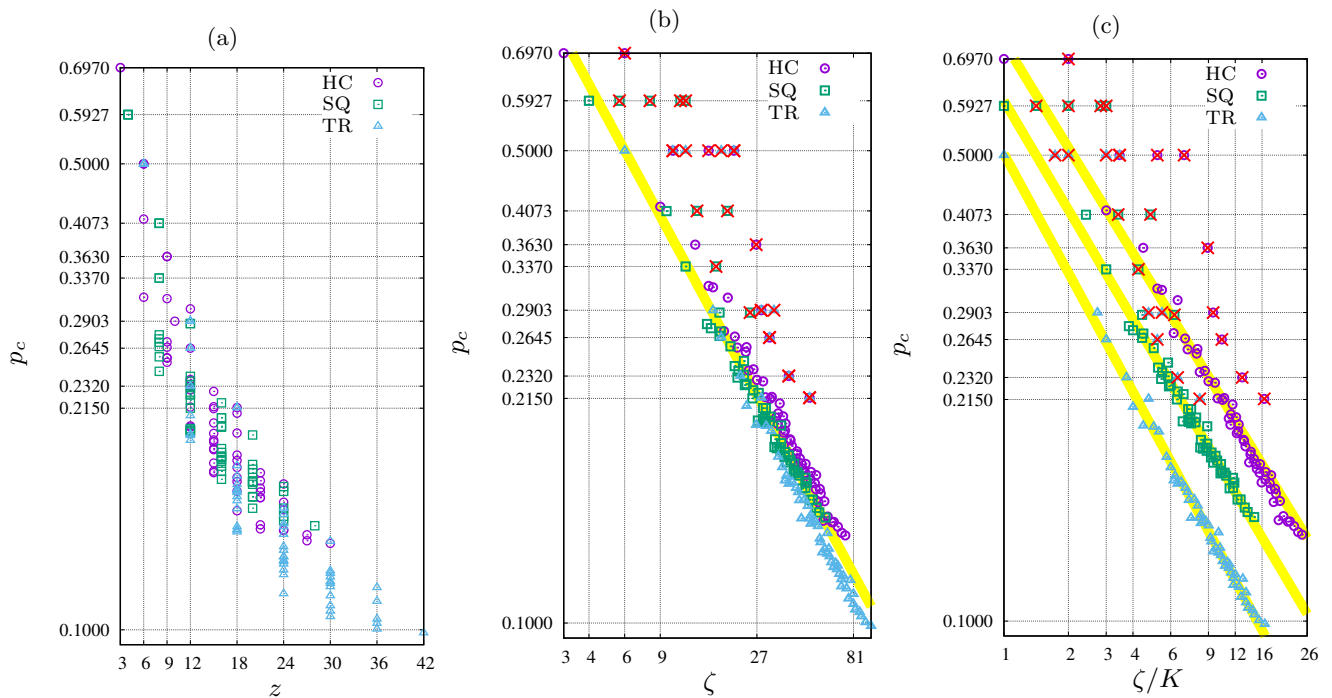


FIG. 4: Percolation thresholds p_c for neighbourhoods containing sites up to the sixth coordination zone on square (\square), honeycomb (\circ) and triangular (\triangle) lattices as dependent on (a) total coordination number z ; (b) index ζ ; (c) index ζ/K . Points marked with crosses (\times) correspond to inflated neighborhoods (such as those collected in Table I), which are excluded from the fitting procedure. The lines show power law fits according to the least-squares method to Equation (9) and Equation (11) on Figures 4(b) and 4(c), respectively

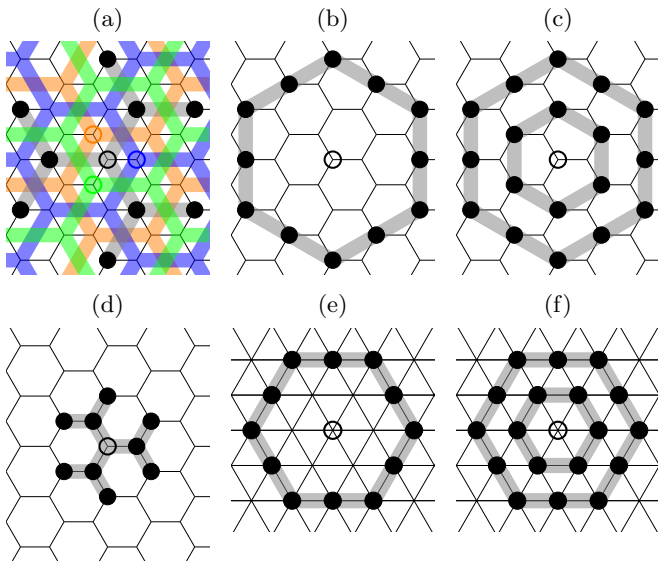


FIG. 5: Inflated complex neighbourhoods (top row) and their lower-index partners (bottom row): (a) HC-3,6 vs. (d) HC-1,2, (b) HC-5,6 vs. (e) TR-2,3 and (c) HC-2,5,6 vs. (f) TR-1,2,3. The neighbourhood HC-3,6 is equivalent to HC-1,2 but with a lattice constant twice as large. This split the system into four independent simultaneously percolating systems

complex neighborhoods: for any combination of the basic ones;

extended neighborhoods: for complex and compact neighborhoods (like SQ-1,2, TR-1,2,3, HC-1,2,3,4, etc.) and

inflated neighbourhoods: for complex neighborhoods reducible to other complex neighborhoods but with lower indexes by shrinking the lattice constant (like those presented in Figure 5 and collected in Table I).

In conclusion, in this paper we estimate percolation thresholds for the random site percolation problem on triangular and honeycomb lattices for neighborhoods containing sites from the sixth coordination zone. The obtained values of p_c satisfy the power law: independently of the underlying lattice (according to $p_c \propto \zeta^{-\gamma}$) or even better for separately considered lattices (according to $p_c \propto (\zeta/K)^{-\gamma}$, where K is the connectivity of the lattice). Currently, the applications of complex neighborhoods on various lattice topologies seem to be most promising in agroecology [14].

ACKNOWLEDGMENTS

The authors thank Hubert Skawina for preparing the figures for Table I in Appendix B in the Supplemental

Material [48]. We gratefully acknowledge Poland's high-performance computing infrastructure PLGrid (HPC Center: ACK Cyfronet AGH) for providing computer facilities and support within computational grant no. PLG/2023/016295.

-
- [1] D. Stauffer and A. Aharony, *Introduction to Percolation Theory*, 2nd ed. (Taylor and Francis, London, 1994).
- [2] B. Bollobás and O. Riordan, *Percolation* (Cambridge UP, Cambridge, 2006).
- [3] M. Sahimi, *Applications of Percolation Theory* (Taylor and Francis, London, 1994).
- [4] H. Kesten, *Percolation Theory for Mathematicians* (Birkhauser, Boston, 1982).
- [5] S. R. Broadbent and J. M. Hammersley, Percolation processes: I. Crystals and mazes, *Mathematical Proceedings of the Cambridge Philosophical Society* **53**, 629 (1957).
- [6] J. M. Hammersley, Percolation processes: II. The connective constant, *Mathematical Proceedings of the Cambridge Philosophical Society* **53**, 642 (1957).
- [7] D. Soto-Gomez, L. Vazquez Juiz, P. Perez-Rodriguez, J. Eugenio Lopez-Periago, M. Paradelo, and J. Koestel, Percolation theory applied to soil tomography, *Geoderma* **357**, 113959 (2020); S. F. Bolandtaba and A. Skauge, Network modeling of eor processes: A combined invasion percolation and dynamic model for mobilization of trapped oil, *Transport in Porous Media* **89**, 357 (2011); S. C. Mun, M. Kim, K. Prakashan, H. J. Jung, Y. Son, and O. O. Park, A new approach to determine rheological percolation of carbon nanotubes in microstructured polymer matrices, *Carbon* **67**, 64 (2014); B. Ghanbarian, F. Liang, and H.-H. Liu, Modeling gas relative permeability in shales and tight porous rocks, *Fuel* **272**, 117686 (2020).
- [8] K. Malarz, S. Kaczanowska, and K. Kulakowski, Are forest fires predictable?, *International Journal of Modern Physics C* **13**, 1017 (2002); N. Guisoni, E. S. Loscar, and E. V. Albano, Phase diagram and critical behavior of a forest-fire model in a gradient of immunity, *Physical Review E* **83**, 011125 (2011); A. Simeoni, P. Salinesi, and F. Morandini, Physical modelling of forest fire spreading through heterogeneous fuel beds, *International Journal of Wildland Fire* **20**, 625 (2011); G. Camelo-Neto and S. Coutinho, Forest-fire model with resistant trees, *Journal of Statistical Mechanics—Theory and Experiment* **2011**, P06018 (2011); S. R. Abades, A. Gaxiola, and P. A. Marquet, Fire, percolation thresholds and the savanna forest transition: A neutral model approach, *Journal of Ecology* **102**, 1386 (2014).
- [9] R. M. Ziff, Percolation and the pandemic, *Physica A* **568**, 125723 (2021).
- [10] B. G. Ueland, N. H. Jo, A. Sapkota, W. Tian, M. Masters, H. Hodovanets, S. S. Downing, C. Schmidt, R. J. McQueeney, S. L. Bud'ko, A. Kreyssig, P. C. Canfield, and A. I. Goldman, Reduction of the ordered magnetic moment and its relationship to Kondo coherence in $\text{Ce}_{1-x}\text{La}_x\text{Cu}_2\text{Ge}_2$, *Physical Review B* **97**, 165121 (2018); L. Keeney, C. Downing, M. Schmidt, M. E. Pemble, V. Nicolosi, and R. W. Whatmore, Direct atomic scale determination of magnetic ion partition in a room temperature multiferroic material, *Scientific Reports* **7**, 1737 (2017); P. Buczek, L. M. Sandratskii, N. Buczek, S. Thomas, G. Vignale, and A. Ernst, Magnons in disordered nonstoichiometric low-dimensional magnets, *Physical Review B* **94**, 054407 (2016); Y. Yiu, P. Bonfá, S. Sanna, R. De Renzi, P. Carretta, M. A. McGuire, A. Huq, and S. E. Nagler, Tuning the magnetic and structural phase transitions of PrFeAsO via Fe/Ru spin dilution, *Physical Review B* **90**, 064515 (2014); M. Grady, Possible new phase transition in the 3D Ising model associated with boundary percolation, *Journal of Physics: Condensed Matter* **35**, 285401 (2023).
- [11] J. Jeong, K. J. Park, E.-J. Cho, H.-J. Noh, S. B. Kim, and H.-D. Kim, Electronic structure change of $\text{NiS}_{2-x}\text{Se}_x$ in the metal-insulator transition probed by X-ray absorption spectroscopy, *Journal of the Korean Physical Society* **72**, 111 (2018); A. Avella, A. M. Oles, and P. Horsch, Defect-induced orbital polarization and collapse of orbital order in doped vanadium perovskites, *Physical Review Letters* **122**, 127206 (2019); L. Cheng, P. Yan, X. Yang, H. Zou, H. Yang, and H. Liang, High conductivity, percolation behavior and dielectric relaxation of hybrid ZIF-8/CNT composites, *Journal of Alloys and Compounds* **825**, 154132 (2020).
- [12] F. Xu, Z. Xu, and B. I. Yakobson, Site-percolation threshold of carbon nanotube fibers—Fast inspection of percolation with Markov stochastic theory, *Physica A* **407**, 341 (2014).
- [13] M. Alguero, M. Perez-Cerdan, R. P. del Real, J. Ricote, and A. Castro, Novel Aurivillius $\text{Bi}_4\text{Ti}_{3-2x}\text{Nb}_x\text{Fe}_x\text{O}_{12}$ phases with increasing magnetic-cation fraction until percolation: A novel approach for room temperature multiferroism, *Journal of Materials Chemistry C* **8**, 12457 (2020); M. Meloni, M. J. Large, J. M. González Domínguez, S. Victor-Román, G. Fratta, E. Istif, O. Tomes, J. P. Salvage, C. P. Ewels, M. Pelaez-Fernandez, R. Arenal, A. Benito, W. K. Maser, A. A. K. King, P. M. Ajayan, S. P. Ogilvie, and A. B. Dalton, Explosive percolation yields highly-conductive polymer nanocomposites, *Nature Communications* **13**, 6872 (2022).
- [14] J. E. Ramírez, C. Pajares, M. I. Martínez, R. Rodríguez Fernández, E. Molina-Gayosso, J. Lozada-Lechuga, and A. Fernández Téllez, Site-bond percolation solution to preventing the propagation of *Phytophthora zoospores* on plantations, *Physical Review E* **101**, 032301 (2020); D. R. Herrera, J. Velázquez-Castro, A. F. Téllez, J. F. López-Olguín, and J. E. Ramírez, Site percolation threshold of composite square lattices and its agroecology applications, *Physical Review E* **109**, 014304 (2024).
- [15] A. Moreira, J. Andrade, and D. Stauffer, Sznajd social model on square lattice with correlated percolation, *International Journal of Modern Physics C* **12**, 39 (2001).

- [16] S. Galam, The September 11 attack: A percolation of individual passive support, *European Physical Journal B* **26**, 269 (2002); S. Galam and A. Mauger, On reducing terrorism power: A hint from physics, *Physica A* **323**, 695 (2003).
- [17] W. Cao, L. Dong, L. Wu, and Y. Liu, Quantifying urban areas with multi-source data based on percolation theory, *Remote Sensing of Environment* **241**, 111730 (2020).
- [18] M. Beddoe, T. Gözl, M. Barkey, E. Bau, M. Godejohann, S. A. Maier, F. Keilmann, M. Moldovan, D. Prodan, N. Ilie, and A. Tittl, Probing the micro- and nanoscopic properties of dental materials using infrared spectroscopy: A proof-of-principle study, *Acta Biomaterialia* **168**, 309 (2023).
- [19] L. Cirigliano, C. Castellano, and G. Timár, Extended-range percolation in complex networks, *Physical Review E* **108**, 044304 (2023).
- [20] G. Liu, Y. Deng, and K. H. Cheong, Network immunization strategy by eliminating fringe nodes: A percolation perspective, *IEEE Transactions on Systems, Man, and Cybernetics: Systems* **53**, 1862 (2023).
- [21] K. Malarz and M. Wołoszyn, Thermal properties of structurally balanced systems on classical random graphs, *Chaos* **33**, 073115 (2023).
- [22] S. Bartolucci, F. Caccioli, and P. Vivo, A percolation model for the emergence of the Bitcoin Lightning Network, *Scientific Reports* **10**, 4488 (2020).
- [23] A. A. Saberi, Recent advances in percolation theory and its applications, *Physics Reports* **578**, 1 (2015).
- [24] M. Li, R.-R. Liu, L. Lü, M.-B. Hu, S. Xu, and Y.-C. Zhang, Percolation on complex networks: Theory and application, *Physics Reports* **907**, 1 (2021).
- [25] M. Sahimi, Explosive percolation and its applications, in *Applications of Percolation Theory* (Springer International Publishing, Cham, 2023) pp. 517–548.
- [26] M.-A. M. Cruz, J. P. Ortiz, M. P. Ortiz, and A. Balankin, Percolation on fractal networks: A survey, *Fractal and Fractional* **7**, 231 (2023).
- [27] Y. Cho and B. Kahng, Discontinuous percolation transitions in cluster merging processes, *Journal of Physics A: Mathematical and Theoretical* **55**, 374002 (2022); M. Li, J. Wang, and Y. Deng, Explosive percolation obeys standard finite-size scaling in an event-based ensemble, *Physical Review Letters* **130**, 147101 (2023); Q. Wu and J. Wang, Thresholds and critical exponents of explosive bond percolation on the square lattice, *International Journal of Modern Physics C* **33**, 2250096 (2022); Z. Luo, W. Chen, and J. Nagler, Universality of explosive percolation under product and sum rule, *Physical Review E* **108**, 034108 (2023); K. Hagiwara and Y. Ozeki, Size-independent scaling analysis for explosive percolation, *Physical Review E* **106**, 054138 (2022).
- [28] S. Galam and A. Mauger, Universal formulas for percolation thresholds, *Physical Review E* **53**, 2177 (1996).
- [29] S. C. van der Marck, Universal formulas for percolation thresholds — Comment, *Physical Review E* **55**, 1228 (1997).
- [30] S. Galam and A. Mauger, Reply to “Comment on ‘Universal formulas for percolation thresholds’”, *Physical Review E* **55**, 1230 (1997).
- [31] S. Galam and A. Mauger, Universal formulas for percolation thresholds. II. Extension to anisotropic and aperiodic lattices, *Physical Review E* **56**, 322 (1997).
- [32] F. Babalievski, Comment on “Universal formulas for percolation thresholds. II. Extension to anisotropic and aperiodic lattices”, *Physical Review E* **59**, 1278 (1999).
- [33] Z. Xun, D. Hao, and R. M. Ziff, Site and bond percolation thresholds on regular lattices with compact extended-range neighborhoods in two and three dimensions, *Physical Review E* **105**, 024105 (2022).
- [34] Z. Xun, D. Hao, and R. M. Ziff, Site percolation on square and simple cubic lattices with extended neighborhoods and their continuum limit, *Physical Review E* **103**, 022126 (2021).
- [35] S. Galam and A. Mauger, A new scheme to percolation thresholds, *Journal of Applied Physics* **75**, 5526 (1994).
- [36] S. Galam and A. Mauger, Site percolation thresholds in all dimensions, *Physica A* **205**, 502 (1994).
- [37] Z. Koza, G. Kondrat, and K. Suszczyński, Percolation of overlapping squares or cubes on a lattice, *Journal of Statistical Mechanics: Theory and Experiment* **2014**, P11005 (2014).
- [38] Z. Koza and J. Poła, From discrete to continuous percolation in dimensions 3 to 7, *Journal of Statistical Mechanics: Theory and Experiment* **2016**, 103206 (2016).
- [39] S. Mitra, D. Saha, and A. Sensharma, Percolation in a distorted square lattice, *Physical Review E* **99**, 012117 (2019).
- [40] S. Mitra, D. Saha, and A. Sensharma, Percolation in a simple cubic lattice with distortion, *Physical Review E* **106**, 034109 (2022).
- [41] S. Mitra and A. Sensharma, Site percolation in distorted square and simple cubic lattices with flexible number of neighbors, *Physical Review E* **107**, 064127 (2023).
- [42] K. Malarz, Percolation thresholds on triangular lattice for neighbourhoods containing sites up to the fifth coordination zone, *Physical Review E* **103**, 052107 (2021).
- [43] K. Malarz, Random site percolation on honeycomb lattices with complex neighborhoods, *Chaos* **32**, 083123 (2022).
- [44] K. Malarz, Random site percolation thresholds on square lattice for complex neighborhoods containing sites up to the sixth coordination zone, *Physica A* **632**, 129347 (2023).
- [45] M. E. J. Newman and R. M. Ziff, Fast Monte Carlo algorithm for site or bond percolation, *Physical Review E* **64**, 016706 (2001).
- [46] V. Privman, Finite-size scaling theory, in *Finite size scaling and numerical simulation of statistical systems*, edited by V. Privman (World Scientific, Singapore, 1990) pp. 1–98.
- [47] D. P. Landau and K. Binder, *A Guide to Monte Carlo Simulations in Statistical Physics*, 3rd ed. (Cambridge University Press, 2009).
- [48] See Supplemental Material at [URL will be inserted by publisher] for A) the mapping of the 6th coordination zone in the honeycomb lattice, into the brick-wall-like square lattice, together with their implementations in C; B) shapes of neighborhoods and associated percolation thresholds; C) scaled probability of belonging to the largest cluster vs. occupation probability.
- [49] P. N. Suding and R. M. Ziff, Site percolation thresholds for Archimedean lattices, *Physical Review E* **60**, 275 (1999).
- [50] S. Galam and K. Malarz, Restoring site percolation on damaged square lattices, *Physical Review E* **72**, 027103 (2005).
- [51] M. Majewski and K. Malarz, Square lattice site percola-

tion thresholds for complex neighbourhoods, *Acta Physica Polonica B* **38**, 2191 (2007).

- [52] K. Malarz, Site percolation thresholds on triangular lattice with complex neighborhoods, *Chaos* **30**, 123123 (2020).
- [53] Z. Xun and D. Hao, Monte Carlo simulation of bond percolation on square lattice with complex neighborhoods, *Acta Physica Sinica* **71**, 066401 (2022), in Chinese.

Appendix A: Procedure boundaries() for TR-6 and HC-6 neighborhoods

Listings 1 and 2 show implementations of boundaries() functions to be replaced in the original Newman–Ziff algorithm. The boundaries() procedures for the simple neighborhoods from SQ-1 to SQ-6 for square lattice are available in Appendix A of Reference 44. The boundaries() procedures for the simple neighborhoods from HC-1 to HC-5 are available in Appendix A of Reference 43.

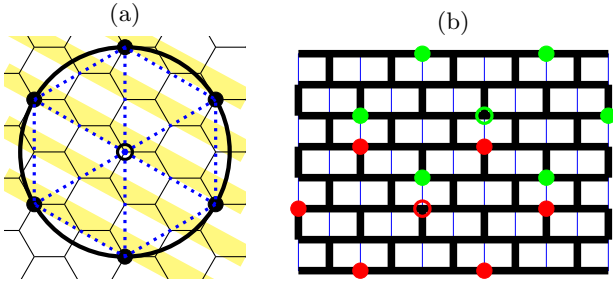


FIG. 6: (a) The sixth coordination zone (HC-6) in the honeycomb lattice, $r^2 = 12$, $z = 6$. (b) Honeycomb lattice mapped into brick-wall like square lattice [49]. Sites with odd and even labels are marked as open red and green circles, respectively. The color fulfilled circles mark sites in the neighborhood. The black horizontal lines correspond to yellow thick lines on panel (a).

Mapping other simple neighborhoods (from HC-1 to HC-5) into brick-wall like square lattice are presented in Figure 3 in Reference 43

Listing 1: boundaries() for TR-6

```

1 // tr-6
2 #define L 2048
3 #define Z 6
4 #define N (L*L)
5
6 int nn[N][Z]; /* Nearest neighbors */
7
8 void boundaries() {
9 int i;
10
11 for(i=0; i<N; i++) {
12 // tr-6 core:
13 nn[i][0]=(N+i-2*L-2)%N;
14 nn[i][1]=(N+i+2*L-4)%N;
15 nn[i][2]=(N+i+4*L-2)%N;

```

```

16 nn[i][3]=(N+i+2*L+2)%N;
17 nn[i][4]=(N+i-2*L+4)%N;
18 nn[i][5]=(N+i-4*L+2)%N;
19 // tr-6 left border:
20 if(i%L==0 || i%L==1) {
21 nn[i][0]=(N+L+i-2*L-2)%N;
22 nn[i][1]=(N+L+i+2*L-4)%N;
23 nn[i][2]=(N+L+i+4*L-2)%N; }
24 if(i%L==2 || i%L==3)
25 nn[i][1]=(N+L+i+2*L-4)%N;
26 // tr-6 right border:
27 if((i+3)%L==0 || (i+4)%L==0)
28 nn[i][4]=(N-L+i-2*L+4)%N;
29 if((i+2)%L==0 || (i+1)%L==0) {
30 nn[i][3]=(N-L+i+2*L+2)%N;
31 nn[i][4]=(N-L+i-2*L+4)%N;
32 nn[i][5]=(N-L+i-4*L+2)%N; }
33 }
34 }

```

Listing 2: boundaries() for HC-6

```

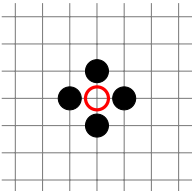
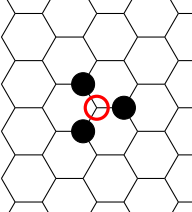
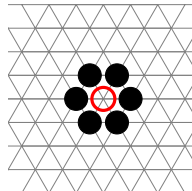
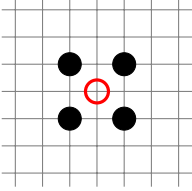
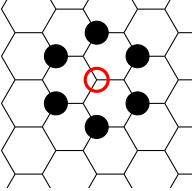
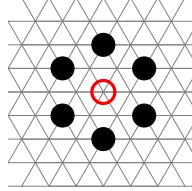
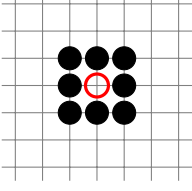
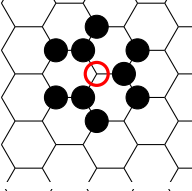
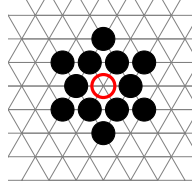
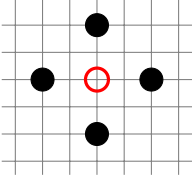
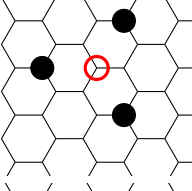
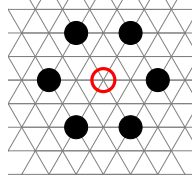
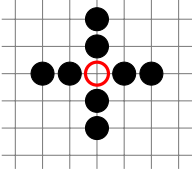
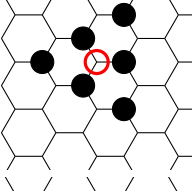
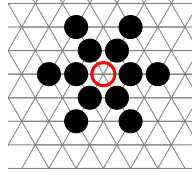
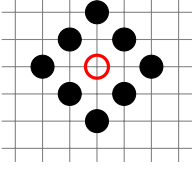
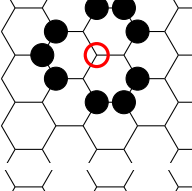
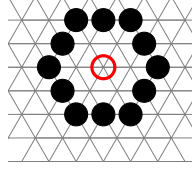
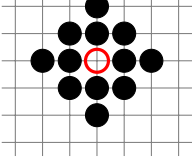
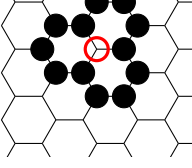
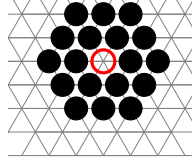
1 // hc-6
2 #define L 2048
3 #define Z 6
4 #define N (L*L)
5
6 int nn[N][Z]; /* Nearest neighbors */
7
8 void boundaries() {
9 int i;
10
11 for(i=0; i<N; i++) {
12 // hc-6 core:
13 nn[i][0] = (N+i -4)%N;
14 nn[i][1] = (N+i +4)%N;
15 nn[i][2] = (N+i +2*L-2)%N;
16 nn[i][3] = (N+i +2*L+2)%N;
17 nn[i][4] = (N+i -2*L-2)%N;
18 nn[i][5] = (N+i -2*L+2)%N;
19 // hc-6 left border:
20 if(i%L==0 || i%L==1 || i%L==2 || i%L==3)
21 nn[i][0] = (N+L+i -4)%N;
22 if(i%L==0 || i%L==1) {
23 nn[i][2] = (N+L+i +2*L-2)%N;
24 nn[i][4] = (N+L+i -2*L-2)%N; }
25 // hc-6 right border:
26 if((i+1)%L==0 || (i+2)%L==0 ||
27 (i+3)%L==0 || (i+4)%L==0)
28 nn[i][1] = (N-L+i +4)%N;
29 if((i+1)%L==0 || (i+2)%L==0) {
30 nn[i][3] = (N-L+i +2*L+2)%N;
31 nn[i][5] = (N-L+i -2*L+2)%N; }
32 }
33 }

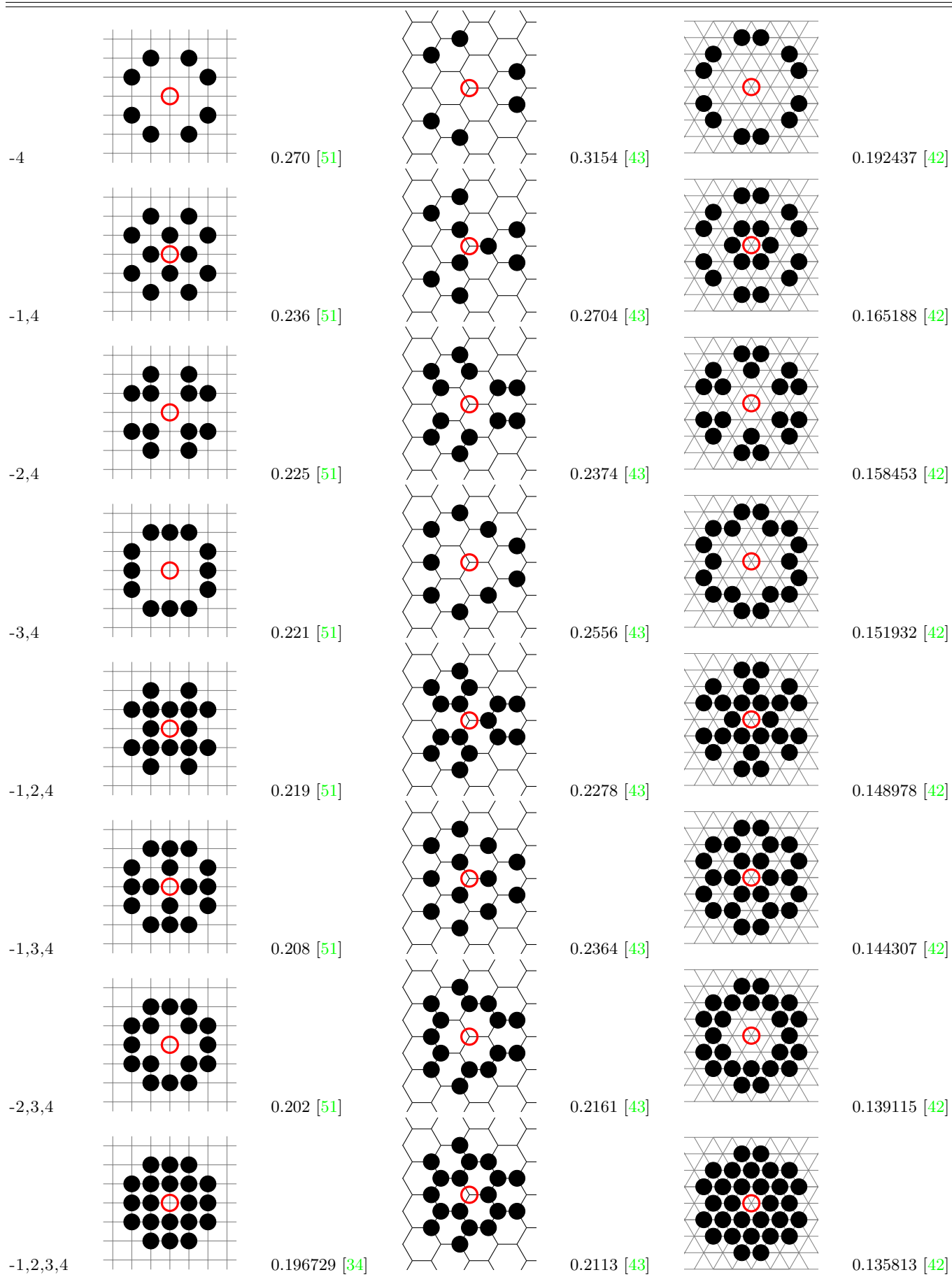
```

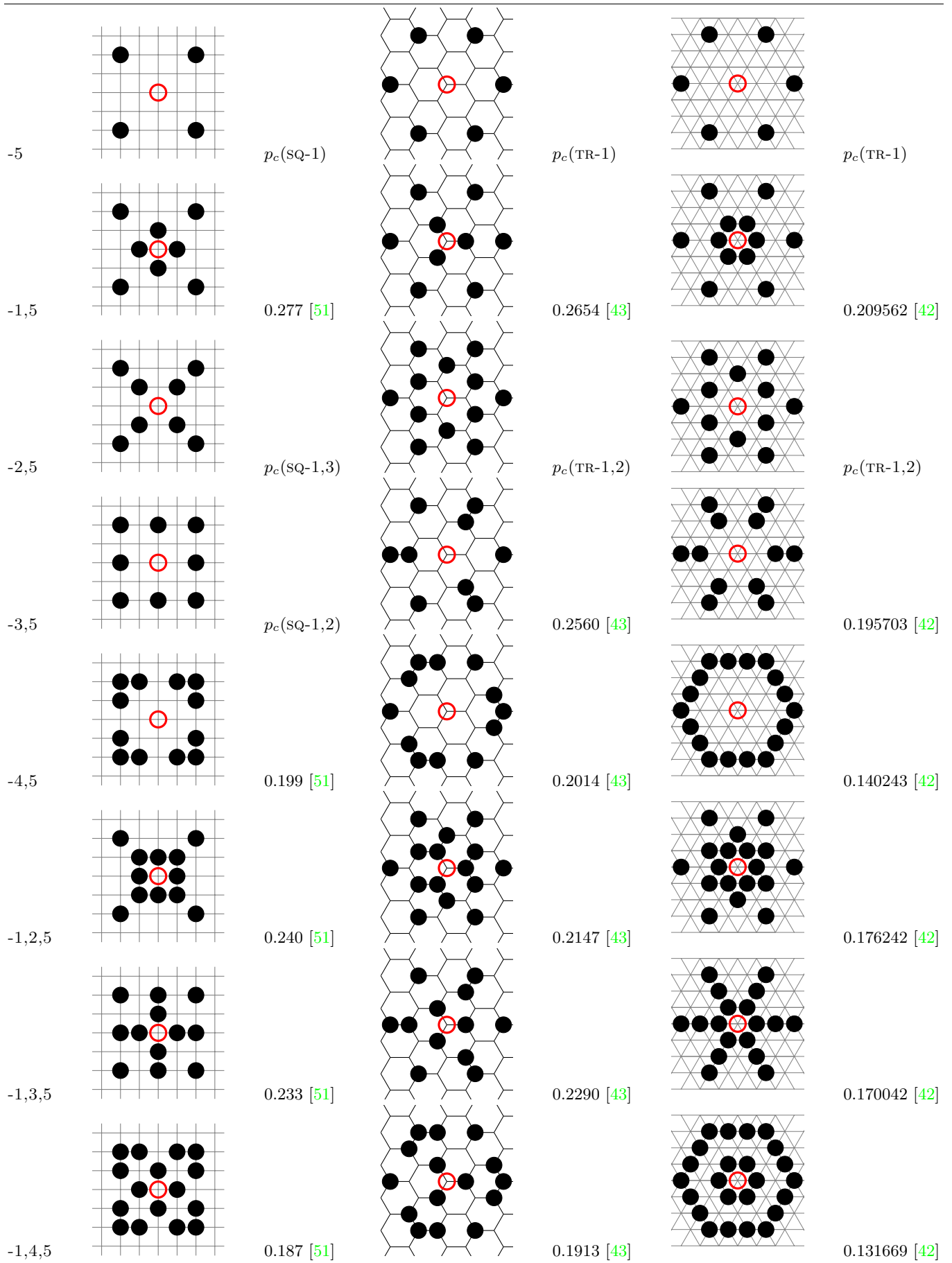
Appendix B: Shapes of neighborhoods and associated percolation thresholds

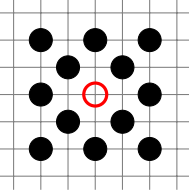
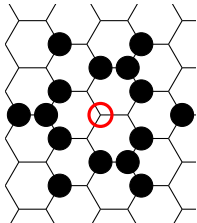
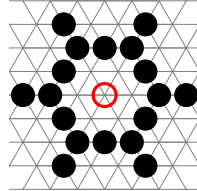
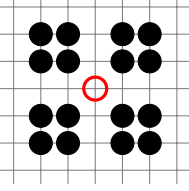
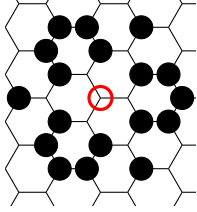
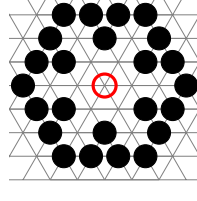
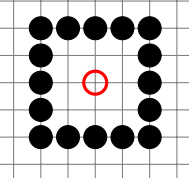
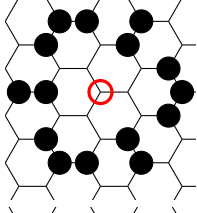
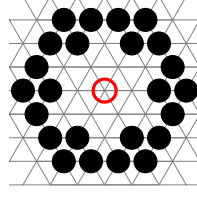
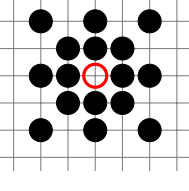
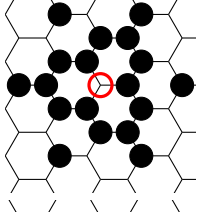
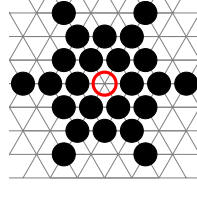
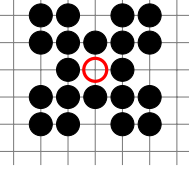
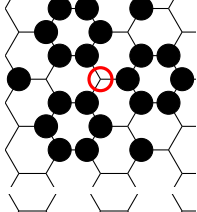
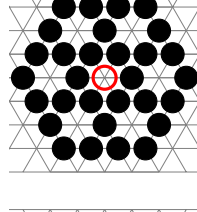
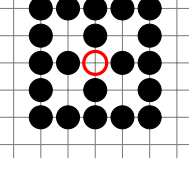
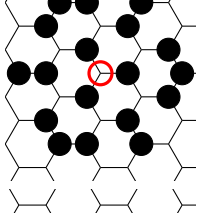
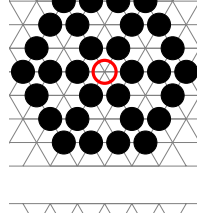
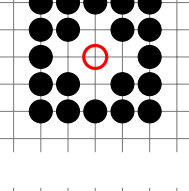
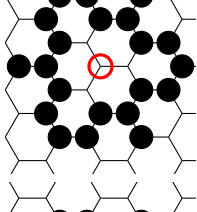
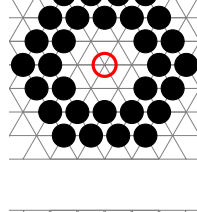
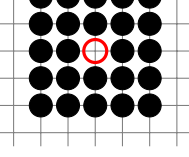
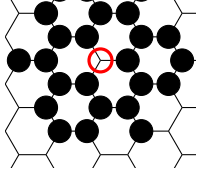
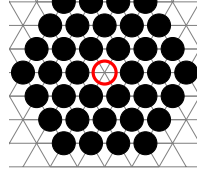
Table II presents shapes of neighborhoods and associated percolation thresholds.

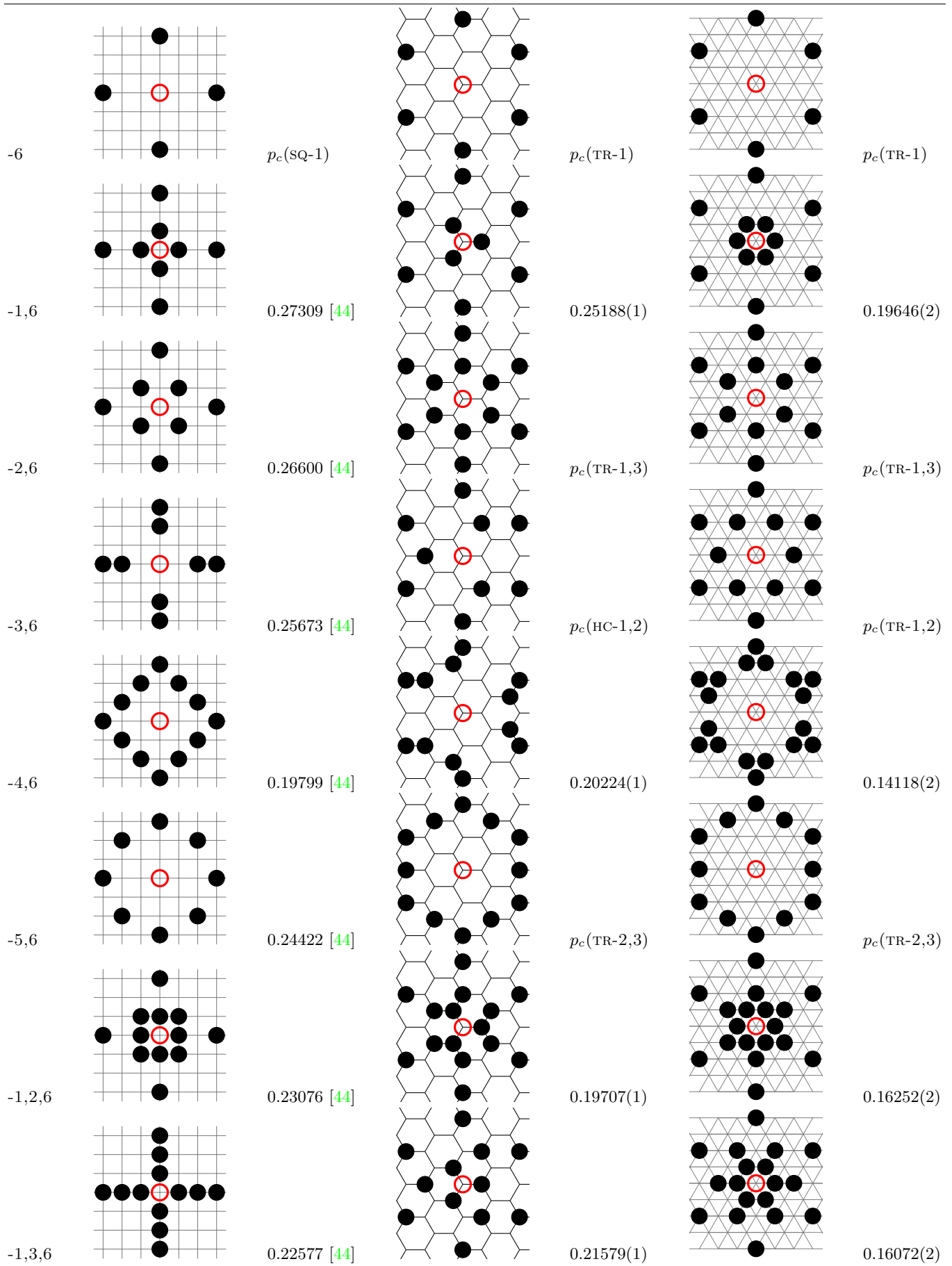
TABLE II: Percolation thresholds p_c for square, honeycomb and triangle lattices and neighborhoods ranging up to the sixth coordination zone

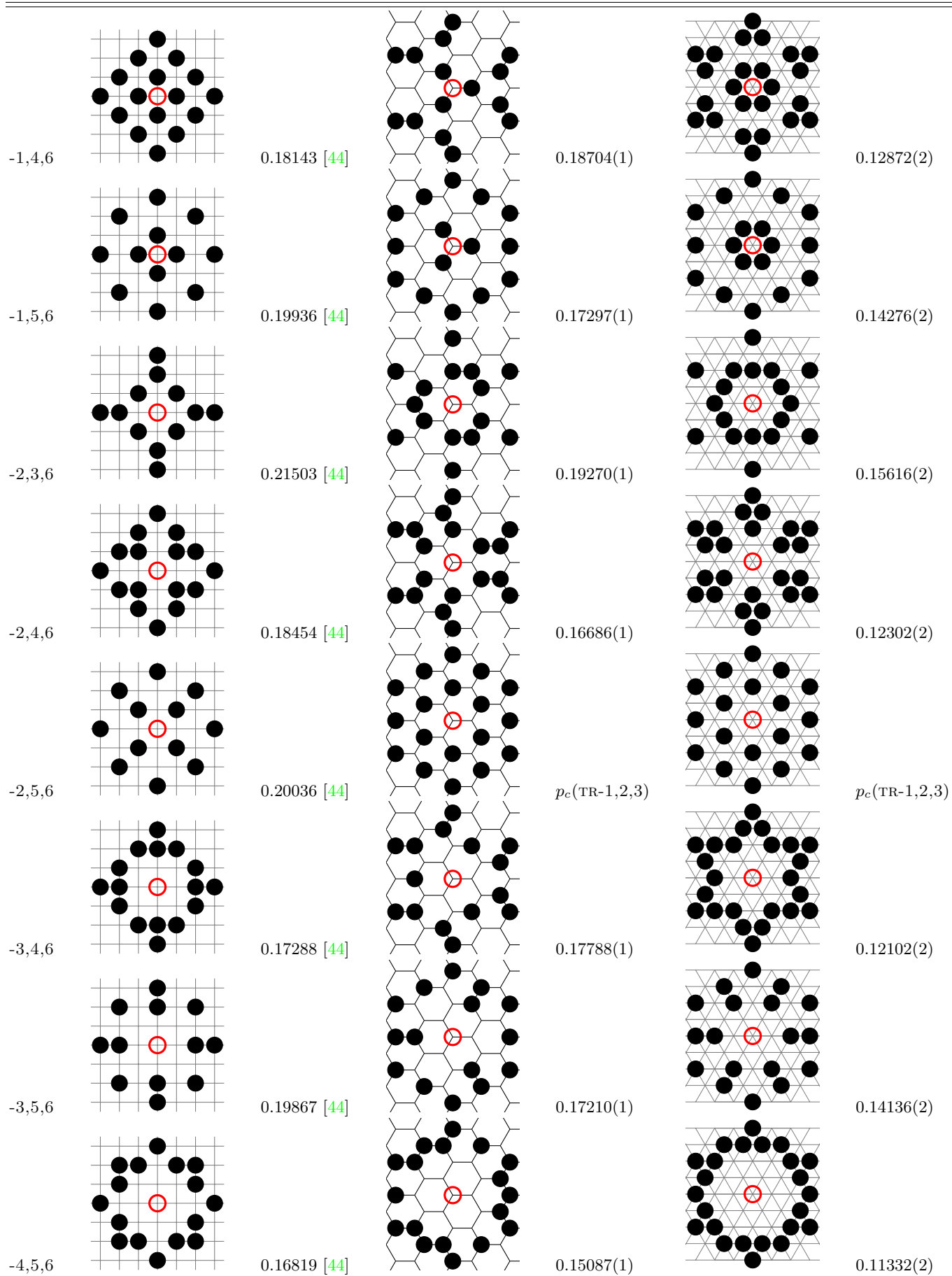
neighborhood	SQ-	p_c	HC-	p_c	TR-	p_c
-1		0.5927460 [1]		0.6970 [1]		1/2 [1]
-2		$p_c(\text{SQ-1})$		$p_c(\text{TR-1})$		$p_c(\text{TR-1})$
-1,2		0.407254 [51]		0.3630 [43]		0.290267 [42]
-3		$p_c(\text{SQ-1})$		$p_c(\text{HC-1})$		$p_c(\text{TR-1})$
-1,3		0.337 [51]		0.4132 [43]		0.264525 [42]
-2,3		$p_c(\text{SQ-1,2})$		0.3139 [43]		0.232012 [42]
-1,2,3		0.288 [50]		0.3030 [43]		0.215462 [42]

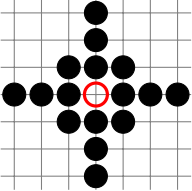
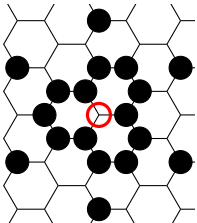
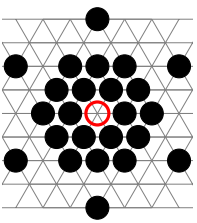
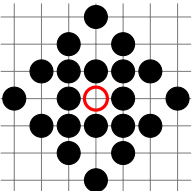
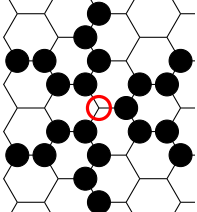
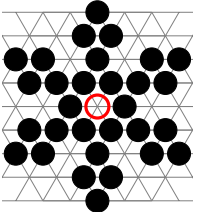
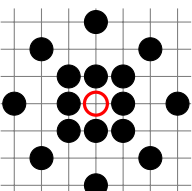
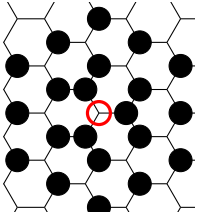
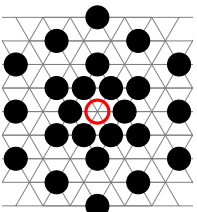
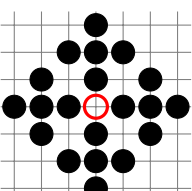
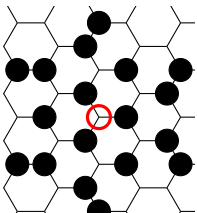
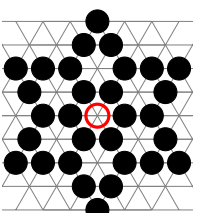
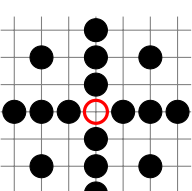
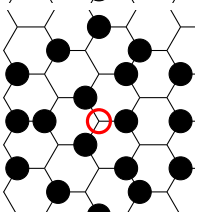
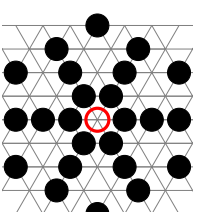
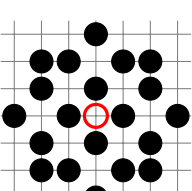
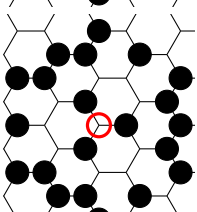
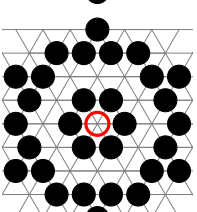
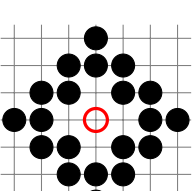
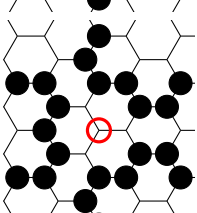
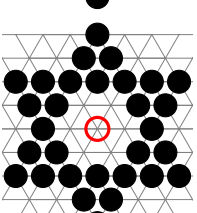
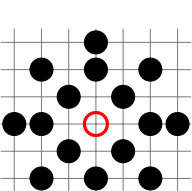
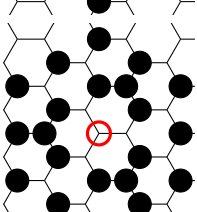
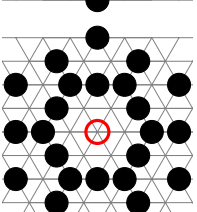


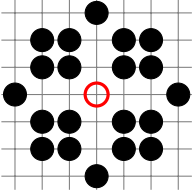
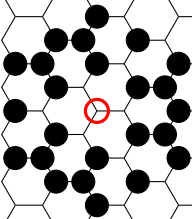
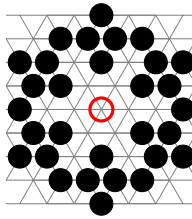
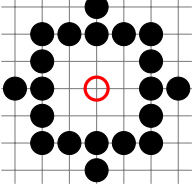
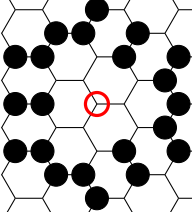
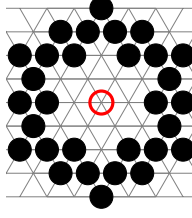
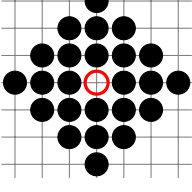
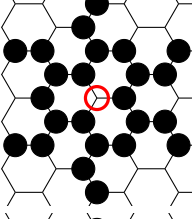
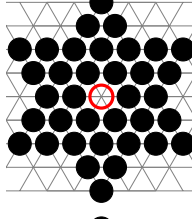
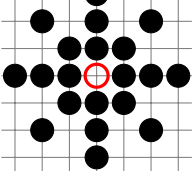
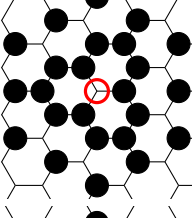
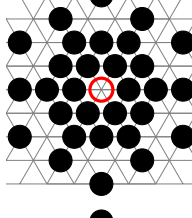
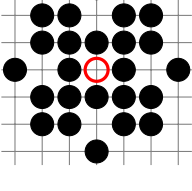
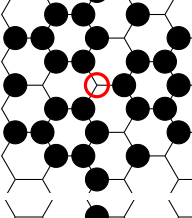
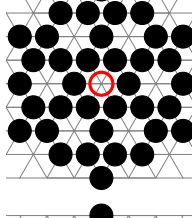
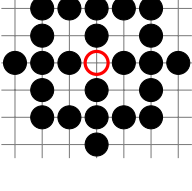
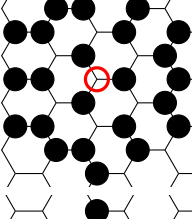
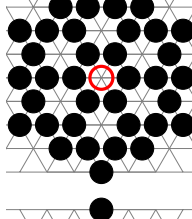
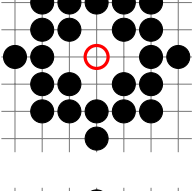
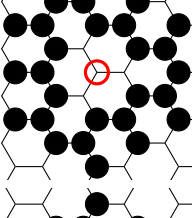
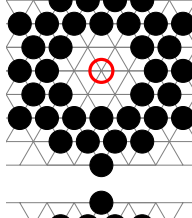
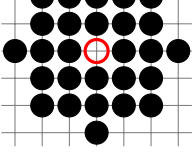
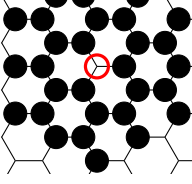
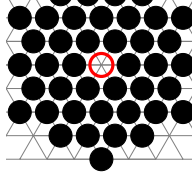


-2,3,5		$p_c(\text{SQ-1,2,3})$		0.2043 [43]		0.161645 [42]
-2,4,5		0.182 [51]		0.1752 [43]		0.126622 [42]
-3,4,5		0.179 [51]		0.1863 [43]		0.125548 [42]
-1,2,3,5		0.208 [51]		0.1973 [43]		0.152259 [42]
-1,2,4,5		0.177 [51]		0.1720 [43]		0.122593 [42]
-1,3,4,5		0.172 [51]		0.1795 [43]		0.121548 [42]
-2,3,4,5		0.167 [51]		0.1673 [43]		0.117440 [42]
-1,2,3,4,5		0.164712 [34]		0.1655 [43]		0.115740 [42]





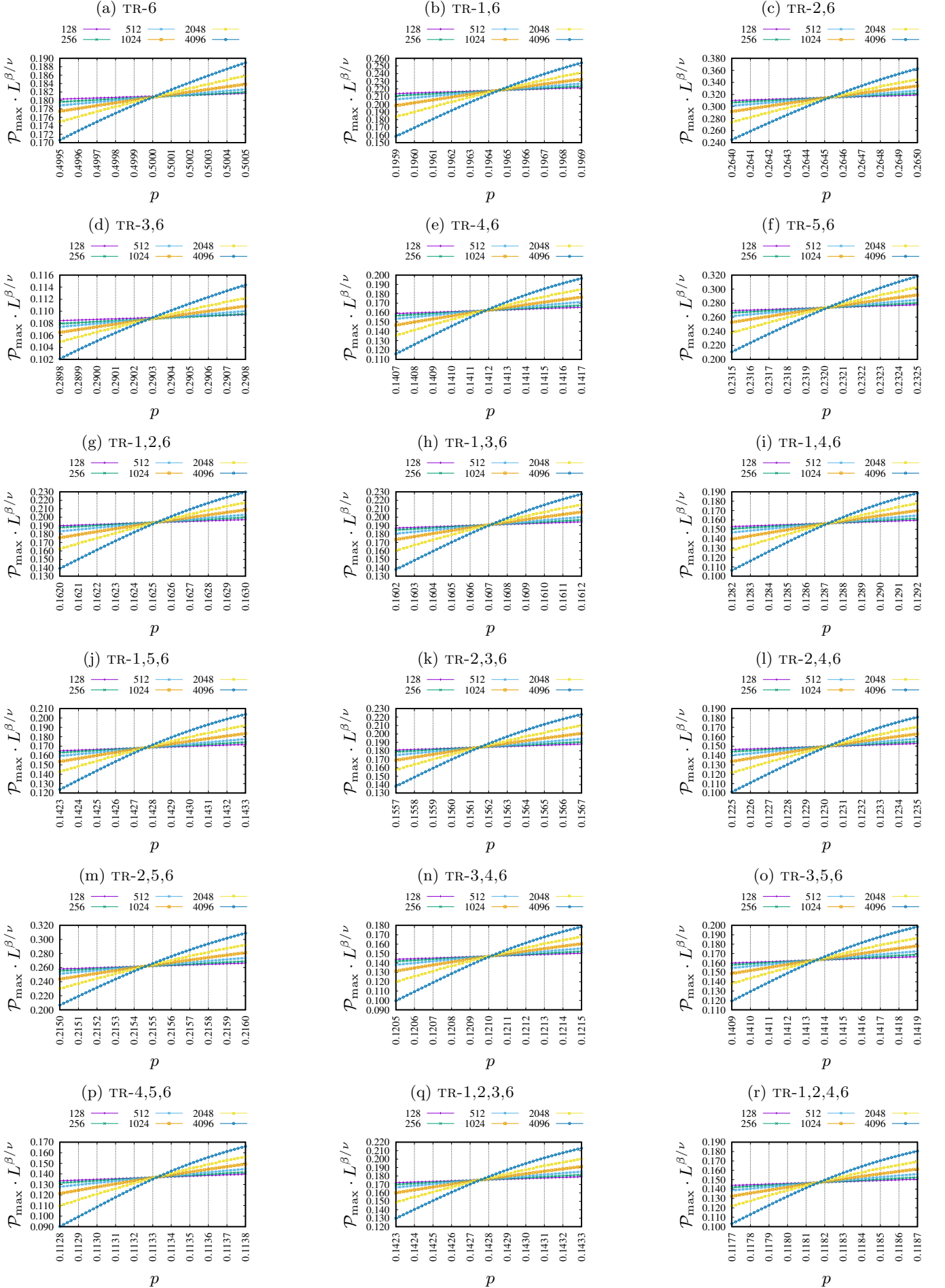
-1,2,3,6		0.20134 [44]		0.18284(1)		0.14276(2)
-1,2,4,6		0.17409 [44]		0.16312(1)		0.11816(2)
-1,2,5,6		0.18216 [44]		0.16102(1)		0.13332(2)
-1,3,4,6		0.16675 [44]		0.16922(1)		0.11612(2)
-1,3,5,6		0.18007 [44]		0.16142(1)		0.12716(2)
-1,4,5,6		0.15815 [44]		0.14710(1)		0.10874(2)
-2,3,4,6		0.16529 [44]		0.15778(1)		0.11254(2)
-2,3,5,6		0.17601 [44]		0.15793(1)		0.12884(2)

-2,4,5,6		0.15844 [44]		0.14113(1)		0.10670(2)
-3,4,5,6		0.15221 [44]		0.14370(1)		0.10466(2)
-1,2,3,4,6		0.16134 [44]		0.15540(1)		0.11042(2)
-1,2,3,5,6		0.16661 [44]		0.15142(1)		0.12008(2)
-1,2,4,5,6		0.15223 [44]		0.13885(1)		0.10374(2)
-1,3,4,5,6		0.14801 [44]		0.14098(1)		0.10232(2)
-2,3,4,5,6		0.14576 [44]		0.13601(1)		0.10030(2)
-1,2,3,4,5,6		0.143255 [34]		0.13480(1)		0.09900(2)

Appendix C: Scaled probability of belonging to the largest cluster vs. occupation probability

probability of occupation p .

Figures 7 and 8 shows scaled (by factor $L^{\beta/\nu}$) probability \mathcal{P}_{\max} of belonging to the largest cluster vs. the



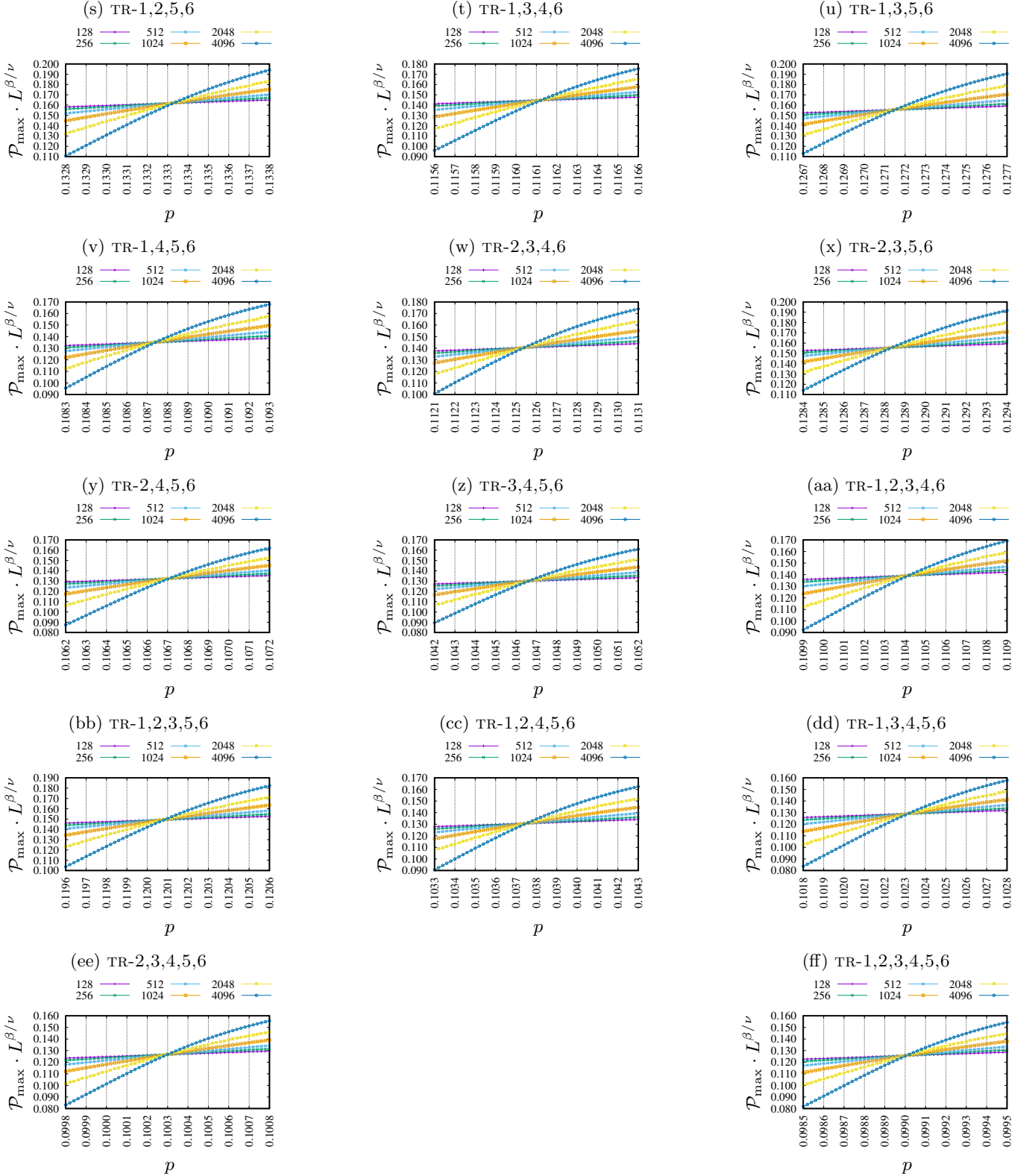
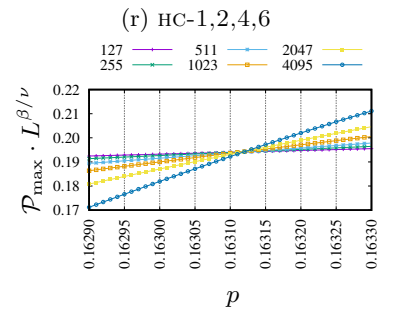
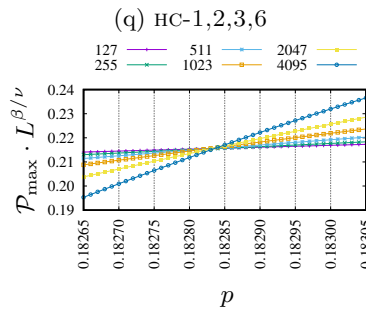
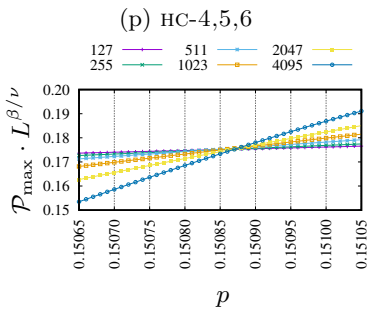
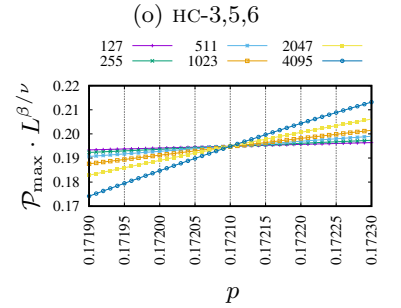
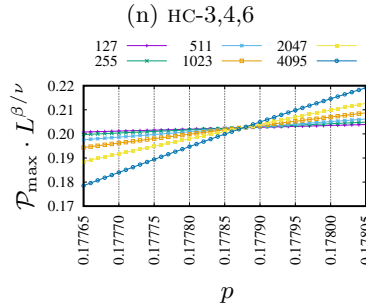
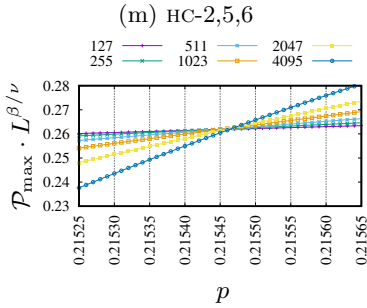
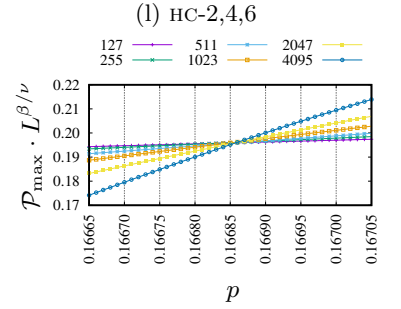
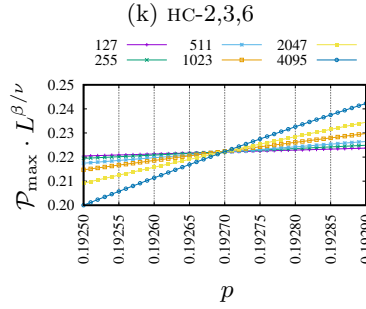
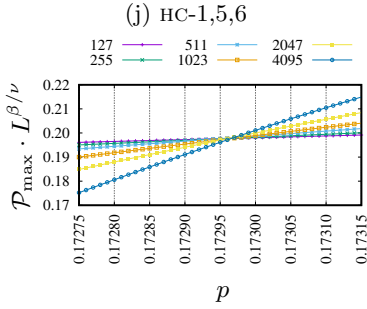
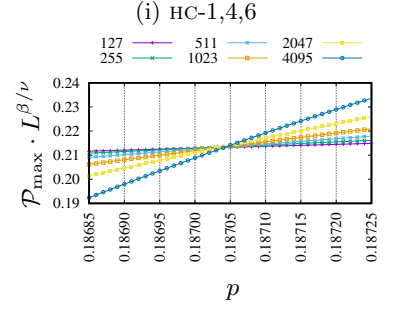
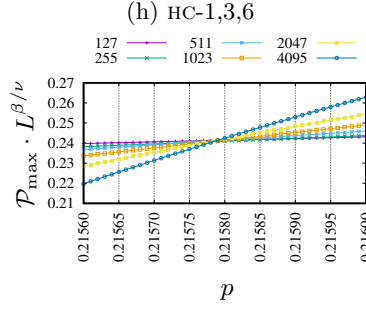
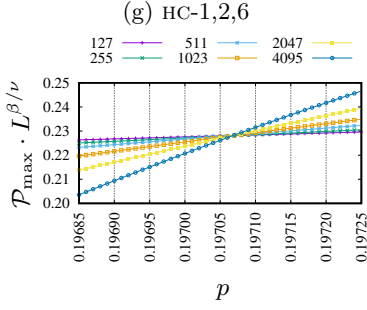
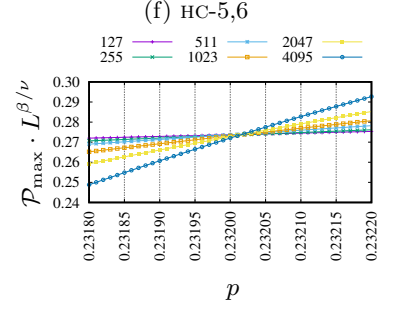
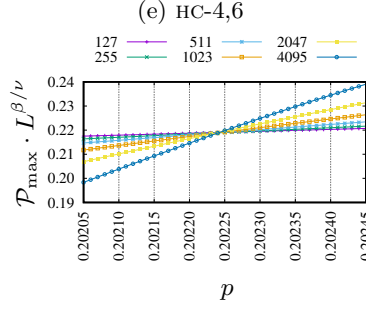
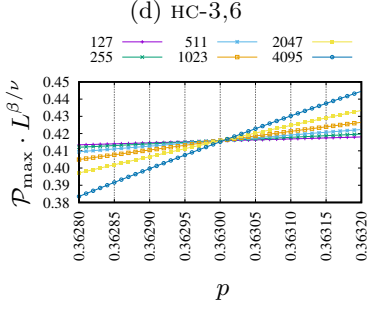
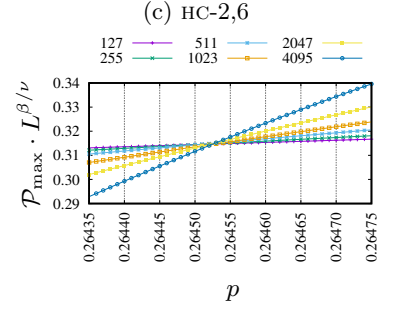
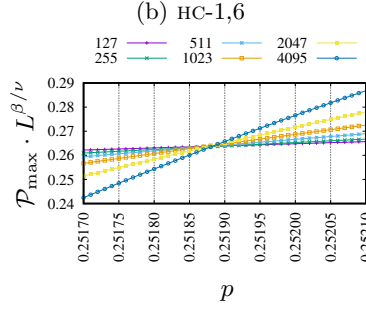
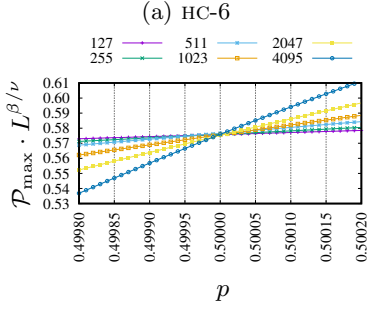


FIG. 7: $\mathcal{P}_{\max} \cdot L^{\beta/\nu}$ vs. p for various complex neighborhoods on triangular lattice. Results are averaged over $R = 10^5$ simulations and $\Delta p = 2 \times 10^{-5}$. (a) TR-6, (b) TR-1,6, (c) TR-2,6, (d) TR-3,6, (e) TR-4,6, (f) TR-5,6, (g) TR-1,2,6, (h) TR-1,3,6, (i) TR-1,4,6, (j) TR-1,5,6, (k) TR-2,3,6, (l) TR-2,4,6, (m) TR-2,5,6, (n) TR-3,4,6, (o) TR-3,5,6, (p) TR-4,5,6, (q) TR-1,2,3,6, (r) TR-1,2,4,6, (s) TR-1,2,5,6, (t) TR-1,3,4,6, (u) TR-1,3,5,6, (v) TR-1,4,5,6, (w) TR-2,3,4,6, (x) TR-2,3,5,6, (y) TR-2,4,5,6, (z) TR-3,4,5,6, (aa) TR-1,2,3,4,6, (bb) TR-1,2,3,5,6, (cc) TR-1,2,4,5,6, (dd) TR-1,3,4,5,6, (ee) TR-2,3,4,5,6, (ff) TR-1,2,3,4,5,6



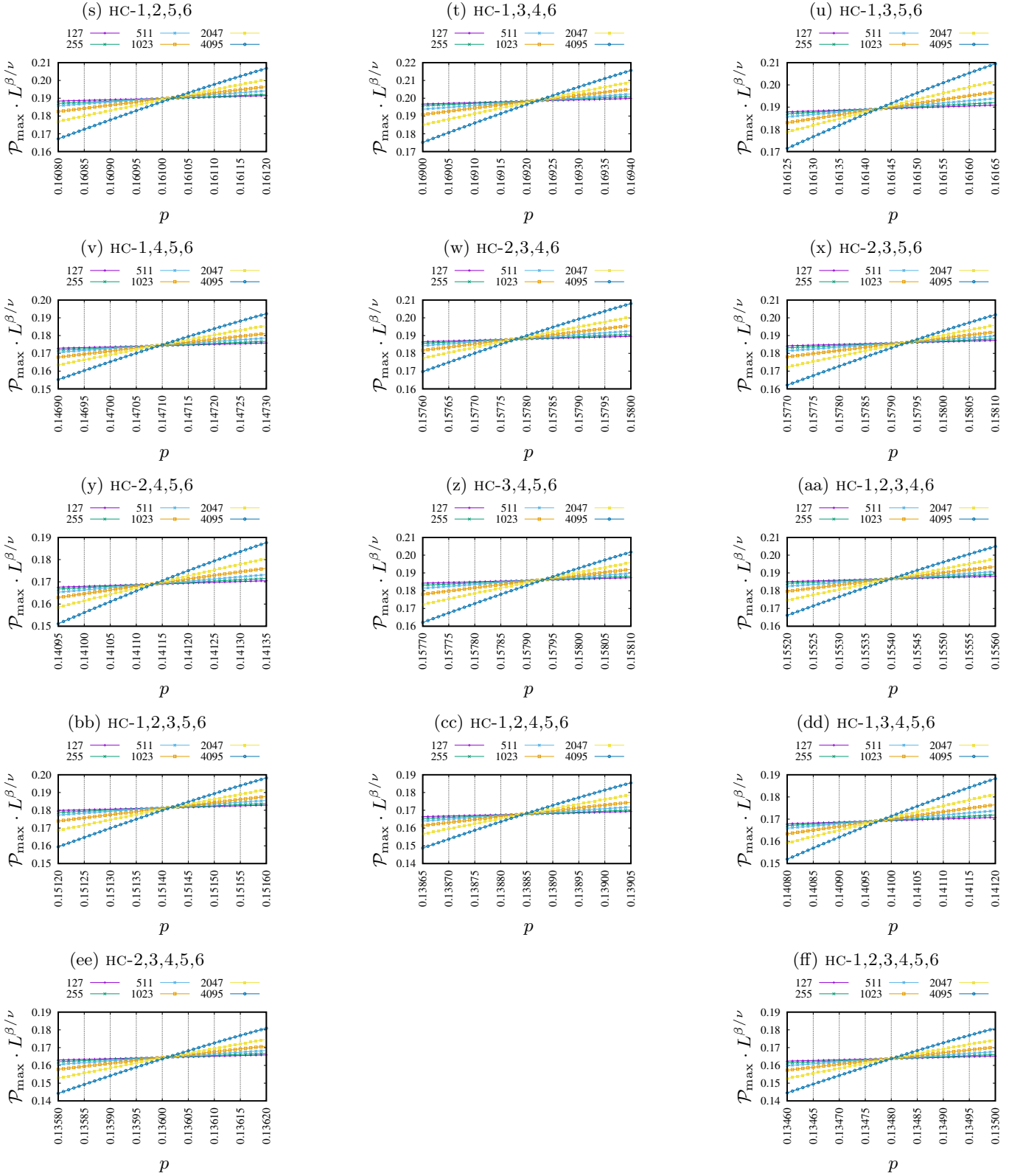


FIG. 8: $\mathcal{P}_{\max} \cdot L^{\beta/\nu}$ vs. p for various complex neighborhoods on honeycomb lattice. Results are averaged over $R = 10^5$ simulations and $\Delta p = 10^{-5}$. (a) HC-6, (b) HC-1,6, (c) HC-2,6, (d) HC-3,6, (e) HC-4,6, (f) HC-5,6, (g) HC-1,2,6, (h) HC-1,3,6, (i) HC-1,4,6, (j) HC-1,5,6, (k) HC-2,3,6, (l) HC-2,4,6, (m) HC-2,5,6, (n) HC-3,4,6, (o) HC-3,5,6, (p) HC-4,5,6, (q) HC-1,2,3,6, (r) HC-1,2,4,6, (s) HC-1,2,5,6, (t) HC-1,3,4,6, (u) HC-1,3,5,6, (v) HC-1,4,5,6, (w) HC-2,3,4,6, (x) HC-2,3,5,6, (y) HC-2,4,5,6, (z) HC-3,4,5,6, (aa) HC-1,2,3,4,6, (bb) HC-1,2,3,5,6, (cc) HC-1,2,4,5,6, (dd) HC-1,3,4,5,6, (ee) HC-2,3,4,5,6, (ff) HC-1,2,3,4,5,6